UNIVERSITY OF CALIFORNIA SAN DIEGO

DMAx: a High-Throughput Computational Tool for Dynamic Mechanical Analysis

A Thesis submitted in partial satisfaction of the requirements
for the Master of Science

in

Materials Science & Engineering

by

Ricardo Silva Buarque

Committee in charge:

Professor Tod Pascal, Chair
Professor Darren Lipomi
Professor Jonathan Pokorski

2023

The Thesis of Ricardo Silva Buarque is approved, and it is acceptable in quality and form for publication on microfilm and electronically.

University of California San Diego

2023

DEDICATION

I would like to dedicate this work to all my middle and high school instructors who instigated my passion for STEM despite all resource limitations of the Brazilian educational system. Not a single experiment, live demonstration, or elaborate class project was necessary: your sheer passion for science conveyed with only chalk, a blackboard, and a strict national entrance exam syllabus, was enough to shape the researcher that I currently am. I hope to, someday, follow in your steps and inspire as many students as you have.

I would also like to dedicate my thesis to the family, friends, and sponsors who were alongside me in this academic journey. Whether by providing a hug, a laugh, or a penny at the right time, you were essential in getting me through my degree.

TABLE OF CONTENTS

LIST OF FIGURES

LIST OF TABLES

LIST OF ABBREVIATIONS

DMA	Dynamic Mechanical Analysis
DMAn	Dynamic Mechanical Analyzer
TTS	Time-Temperature Superposition
MD	Molecular Dynamics
PVDF	Polyvinylidene Fluoride
OPLS-AA	Optimized Potentials for Liquid Simulations – All-Atom
MC	Master Curve
LAMMPS	Large-scale Atomic/Molecular Massively Parallel Simulator
Tg	Glass Transition Temperature
SM	Storage Modulus
LM	Loss Modulus
LT	Loss Tangent
SMILES	Simplified Molecular-Input Line-Entry System
FF	Forcefield

ACKNOWLEDGEMENTS

I would like to acknowledge Professor Tod Pascal for their support as the chair of my committee. Through multiple drafts and many long nights, their guidance has proved to be invaluable.

Chapter 1, in full, is currently being prepared for submission for publication of the material. Silva Buarque, Ricardo; Fune, Beneen; Jamnuch, Sasawat; Ravisankar, Aishwarya; Pascal, Tod. The thesis author was the primary researcher and author of this material.

Chapter 2, in full, is currently being prepared for submission for publication of the material. Silva Buarque, Ricardo; Fune, Beneen; Jamnuch, Sasawat; Ravisankar, Aishwarya; Pascal, Tod. The thesis author was the primary researcher and author of this material.

VITA

2021 Bachelor of Science in Energy Engineering, University of California Berkeley

2023 Master of Science in Materials Science & Engineering, University of California San Diego

ABSTRACT OF THE THESIS

DMAx: a High-Throughput Computational Tool for Dynamic Mechanical Analysis

by

Ricardo Silva Buarque

Master of Science in Materials Science & Engineering

University of California San Diego, 2023

Professor Tod Pascal, Chair

Dynamic Mechanical Analysis (DMA) is an important experimental characterization technique for the mechanical properties of polymers. In this paper, we translate such a technique into a Molecular Dynamics (MD) simulation workflow capable of outputting properties from DMA within a much wider frequency and temperature range than what can be experimentally observed. We also introduce metrics for convergence of simulation runtime and DMA straining size that are not discussed in comparable computational literature but that drastically affect the accuracy of results. We validate the efficacy of the work by comparing our obtained storage and loss modulus data on Polyvinylidene Fluoride (PVDF) with previous computational literature and indicating performance and accuracy improvements for such study based on our convergence metrics. Finally, we perform a complete workflow run at

GHz-range frequencies on PVDF utilizing the All-Atom Optimized Potential for Liquid Simulations (OPLS-AA). With this, we hope to validate and justify this forcefield as a good standard for high-throughput analyses on other polymers with the workflow and to compare our data with experimental results employing the Time-Temperature Superposition (TTS) method.

INTRODUCTION

The study of material behavior under dynamic conditions is paramount across a wide spectrum of scientific and engineering disciplines. Comprehending the intricate mechanical properties of compounds when subjected to varying temperature, frequency, and strain rates is crucial in designing and optimizing novel materials for cutting-edge applications. Dynamic Mechanical Analysis (DMA) is a powerful and versatile experimental technique to investigate the dynamic responses of materials, offering valuable insights into their viscoelastic and mechanical behavior over a wide range of conditions.

The standard operation of a Dynamic Mechanical Analyzer (DMAn) or Rheometer consists of the application of a small periodic stress into a polymeric sample with a defined frequency and under controlled temperature conditions. Such oscillatory stress will generate a strain response in the material at the same frequency as the stimulus applied. A perfectly elastic material will have its sinusoidal stress perfectly matching the applied strain. On the other hand, a perfectly viscous material should have an exact phase angle between the sinusoidal strain applied and the observed pressure response of 90°. A viscoelastic material should have an intermediate behavior, with a phase lag in its stress response between 0° and 90° [1]. These behaviors are depicted in Figure 0.1.

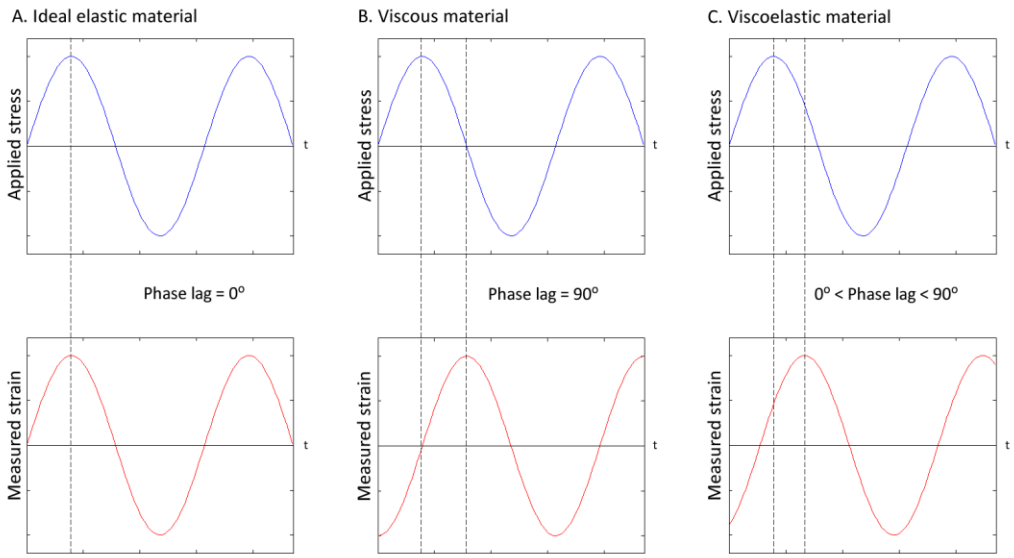

Figure 0.1.1: Periodic stress/strain response from a material under Dynamic Mechanical Analysis. Adapted from [1]

The most important dynamic mechanical information extracted from these periodic stress-strain results are the Storage Modulus (SM), the Loss Modulus (LM), and the Loss Tangent (LT) for the analyzed species. These properties are obtained by multiplying the ratio of the maximum stress (σ_{max}) and maximum strain (ε_{max}) applied on the material by a trigonometric relation with the phase angle (θ) between the applied strain and the stress response curves (Equations 1.1-1.3). The storage modulus represents the material's ability to store elastic energy and is associated with the material's stiffness. It is generally frequency-dependent, showing variations with the loading rate. The loss modulus indicates the energy dissipated by the material as heat during deformation and characterizes its damping capacity. It also varies with frequency and temperature. The loss tangent is the ratio of the loss modulus to the storage modulus, representing the material's damping behavior, and it provides insights into the material's energy dissipation capabilities [2].

$$SM = \frac{\sigma_{max}}{\varepsilon_{max}} \cos\theta \text{ (Equation 1.1)}$$

$$LM = \frac{\sigma_{max}}{\varepsilon_{max}} \sin\theta \text{ (Equation 1.2)}$$

$$LT = \frac{LM}{SM} = \frac{sin\theta}{cos\theta} = \tan\theta \text{ (Equation 1.3)}$$

Through the evaluation of these moduli against varying time, temperature, and frequency, one can investigate phenomena such as viscoelasticity, glass transition, relaxation behavior, and damping capacity, among other mechanical properties, with DMA. Despite the efficacy of this technique, traditional experimental DMA methods suffer from a series of physical limitations. For instance, the energy necessary to overcome the inertia of the instrument utilized for applying the oscillating stress can be transferred to the sample in the form of heat and cause difficulty in maintaining the sample's temperature constant. The temperature is usually controlled by a heat chamber in which the sample is immersed during the oscillatory behavior of the DMAn, which has a limited temperature range and can fail in keeping the sample temperature constant for more viscous materials under higher-frequency stress. Such chambers are also only responsible for controlling temperature, with no Rheometer to date containing any type of pressure control. In addition, any imprecision in the sample's dimensional measurements is extremely impactful over the measurements of its properties since they exhibit a high geometry dependence. Finally, there are limitations to the frequency-based techniques in DMA since most devices can only perturb the material at up to 1 kHz rates [3]. Therefore, there is little to no data on the mechanical properties of polymers in the high-frequency regime, which has gained immense relevance over the past few decades due to the interest in ultrasound-responsive drug delivery [4] and MHz to GHz-range electronic signal emission and processing [5].

To overcome the high-frequency limitations of DMA, researchers have made use of the Time-Temperature Superposition (TTS) principle observed in polymers to extrapolate data to higher frequencies. TTS suggests that the dynamic mechanical response of a polymer at different frequencies follows an Arrhenius behavior and can be translated to predict its behavior at other unmeasured frequencies (Figure 0.2). This principle is applicable over a broad frequency range, enabling researchers to extend the viscoelastic data obtained from short-term experiments to long-term behaviors - and vice versa - into a Master Curve (MC).

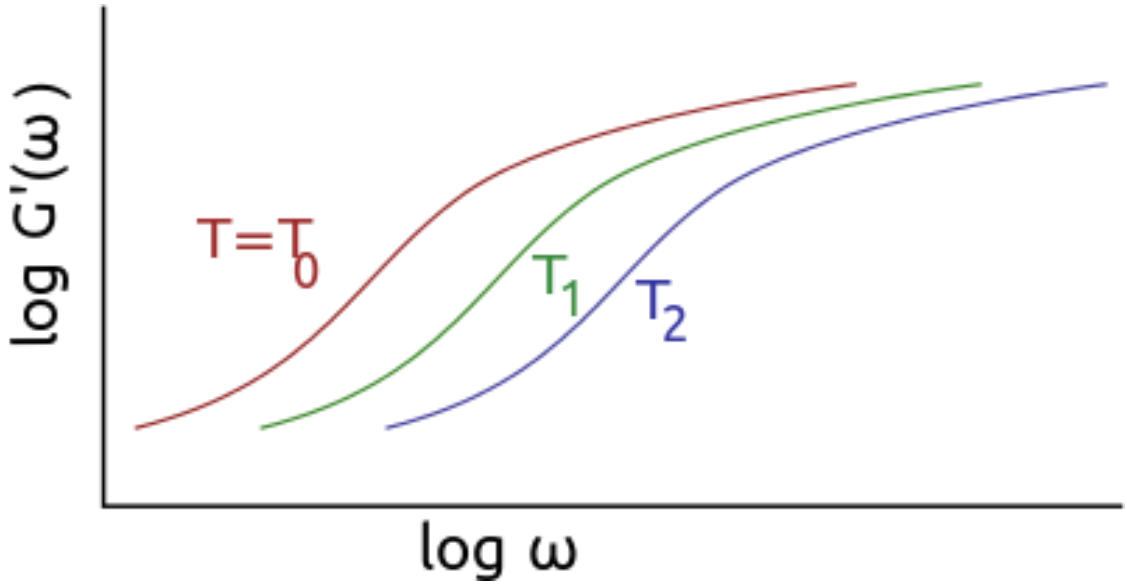

Figure 0.1.2: Temperature dependence of Storage Modulus of a viscoelastic material under periodic excitation. The frequency is ω, G' is the SM, and T0 < T1 < T2. Adapted from [6]

Despite the usefulness of this extrapolation method, it is difficult to validate the high-frequency data since no experiments can be run at such a range. In addition, MCs require several data points - optimally over 100 - of DMAs from multiple frequencies and temperatures, which can be extremely time-consuming at the low-frequency regime. Therefore, in this paper, we introduce a first-of-its-kind computational workflow capable of mimicking the capabilities of a DMAn through Molecular Dynamics simulations. The workflow is equipped with a proxy

designed to select the appropriate number of dynamic cycles to be run in a polymer system and the appropriate strain size for each structure to minimize disparities from experimental conditions, something unique to date in all literature attempts of simulating periodic mechanical properties with MD. It can also simulate several data points for the construction of a Master Curve. Since the workflow can effectively simulate frequencies from the high-kHz regime and above, it is also extremely useful both in validating MCs constructed experimentally and in extrapolating computational data to the low-frequency regime so that it can be validated over empirical measurements. The individual tasks from the workflow can determine several other important parameters of polymers, such as the Young's modulus, the glass temperature, and the storage modulus/loss modulus/loss tangent at specified temperatures, pressures, and frequencies. Finally, the high-throughput capabilities of this workflow open a plethora of possibilities in materials discovery and analysis, whether by aiding in database screening for optimal mechanical properties or by allowing the development of datasets for machine-learned models to suggest new polymeric systems with intrinsic mechanical characteristics.

Chapter 1 Methods & Workflow Description

In this study, all MD simulations were performed with the Large-scale Atomic/Molecular Massively Parallel Simulator (LAMMPS) software. We perform all analyses on an amorphous sample of Polyvinylidene Fluoride (PVDF), built with an in-house script to closely match the system studied by Ghajar et. Al. [7] to validate the efficacy of the workflow and suggest improvements on previous literature. The system, depicted in Figure 1.1, is composed of a set of 10 chains of 100 monomers (6080 atoms) wrapped in periodic boundary conditions with an initial density of 1.68 g/cm^3 to closely match the experimental density of amorphous PVDF [8]. The nonpolar forcefield by Byutner and Smith [9] was used to match the simulation standards most closely from Ghajar [7].

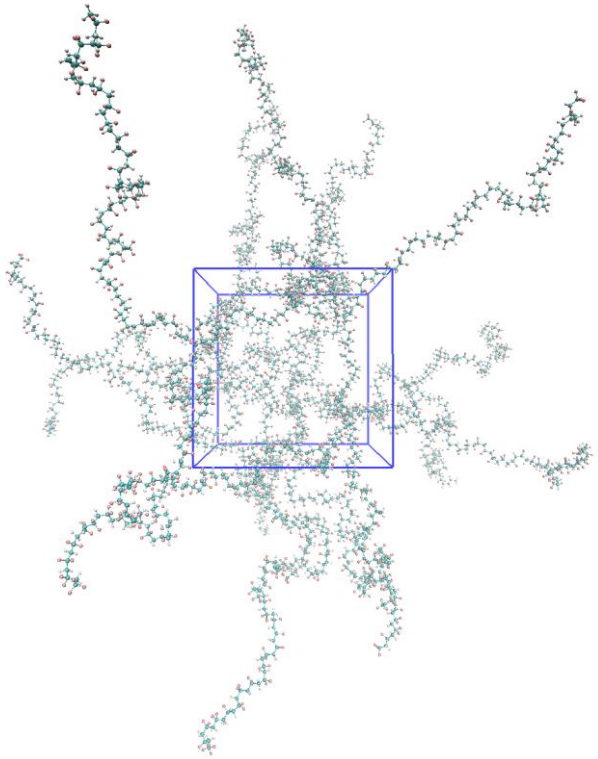

Figure 1.1: PVDF amorphous structure

Equipped with the right input structure and DMA parameters, one can easily navigate the DMAx object-oriented Python package and calculate the storage and loss moduli as well as the loss tangent at a specific temperature, pressure, and frequency for a previously parametrized material. However, to enable high-throughput analysis of multiple polymers as well as detailed property investigation – Young's modulus, glass transition temperature, and master curve of the studied polymer - we have developed a primary workflow that runs sequentially with minimal user interference, depicted in Figure 1.2. We utilize the *jobflow* Python package by Ganose et al. to automate this sequence of tasks. Details about the workflow procedure are described in the following sections.

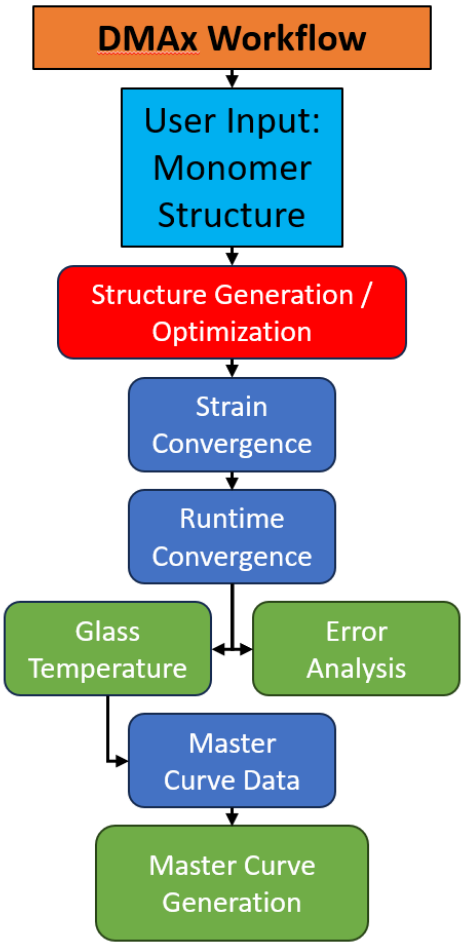

Figure 1.2: DMAx workflow

Input Selection & Structure Optimization

Despite utilizing an externally built structure for this study, we have provided a plethora of options for users to create their polymer systems in DMAx. For simpler polymer systems, we integrate our workflow with Sahu et al.'s [10] *PolymerStructurePredictor* Python package. In this case, users need only to provide a Simplified Molecular-Input Line-Entry System (SMILES) string of the desired monomer and the workflow will build crystalline and amorphous LAMMPS data of it. Parameters such as the density, the number of monomers, and the number of polymer chains can also be input but are otherwise set to values that ensure the highest result accuracy based on training use of the software.

An example of the above standards is that we set a minimum of 6000 atoms for stress data reliability. As further explained later in this section, the storage and loss moduli data are obtained through an analysis of the average pressure response of the system throughout the simulation. Pressure in molecular dynamics simulations is a statistical quantity calculated based on the momentum exchange between particles. In smaller systems, the statistical accuracy of pressure calculations might be lower due to the limited number of particles contributing to this exchange, leading to larger fluctuations. In addition, systems with fewer atoms typically have a higher ratio of surface area to volume. This imbalance can affect the system's response to pressure changes, leading to more pronounced fluctuations compared to larger systems where the ratio of surface area to volume is smaller, hence the need for an established minimum number of atoms for ensuring data quality.

Another standard characteristic of the workflow is to utilize OPLS-AA forcefield parameters as default when no forcefield is specified. We do so because this force field has demonstrated good agreement with experimental data on various polymer properties such as conformational energies, bond lengths, dihedral angles, and phase behavior. In addition, OPLS-

AA provides a balanced representation of bonded and non-bonded interactions within polymer chains. This balance is crucial for accurately capturing the structural and dynamical properties of polymer systems, especially considering intra- and -inter-molecular interactions under periodic strain.

Users are also allowed to enter any MSI Biograf Format (.bgf) or Protein Data Bank (.pdb) structure and any Cerius2-formatted forcefield as the primary inputs for the DMA simulations. Our in-house scripts can parse such files and generate LAMMPS input and data files for the simulations. The user can additionally choose to manually provide the LAMMPS data file desired to be used throughout the workflow. These advanced input tools allow users to amplify the range of structures being studied, such as polymers with impurities or varied groups of polymer chains. They also allow for accuracy improvements as users can provide the most appropriate forcefields for their materials, including better-parametrized machine-learned forcefield options. As will be discussed in the Future Work section, we hope to encode a universal machine-learned forcefield for polymers into DMAx, as well as a tool for properly creating semicrystalline polymer structures besides the crystalline and amorphous tools already available.

Every MD simulation executable in the workflow can subject the polymer to an equilibration sequence of steps before the calculation of its dynamic mechanical properties. For a full run of the workflow, this equilibration set of steps is done only once and the equilibrated structure is saved and utilized as a starting point in further steps to reduce computational cost.

Such equilibration protocol consists of a 500-step conjugate-gradient minimization of the structure, followed by a 10-picosecond heating process from 1K to the desired temperature, utilizing a Nosé-Hoover Thermostat (NVT). Commonly, MD studies start equilibrating materials

already at the desired temperature of analysis, but we utilize this ramping temperature technique to avoid inadequate dynamics caused by a potentially unstable configuration being assigned high atom velocities from start. The material is then subjected to a 1-nanosecond Nosé-Hoover Barostat (NPT) to allow for the density of the system to reach equilibrium. Finally, the lattice parameters are averaged from the NPT step and a final NVT is run for 500 picoseconds to equilibrate the new density at the simulated temperature. Figures 1.3 and 1.4 illustrate the Total Energy and Density of the PVDF system as a function of time with these equilibration steps labeled, indicating the stability of the density after the volume convergence. The Byutner and Smith forcefield [9] underestimates the PVDF density to 1.455 g/cm^3 while OPLS-AA overestimates it at 1.89 g/cm^3, indicating that the OPLS-AA likely weights van der Waals (vdW) interactions stronger between the polymer chains.

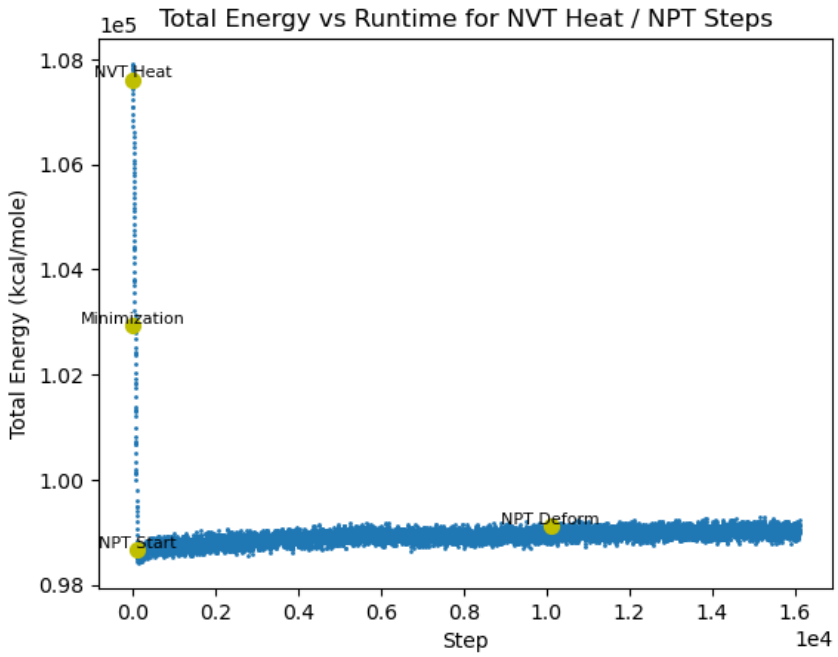

Figure 1.3: Total Energy vs Runtime for the equilibration procedure

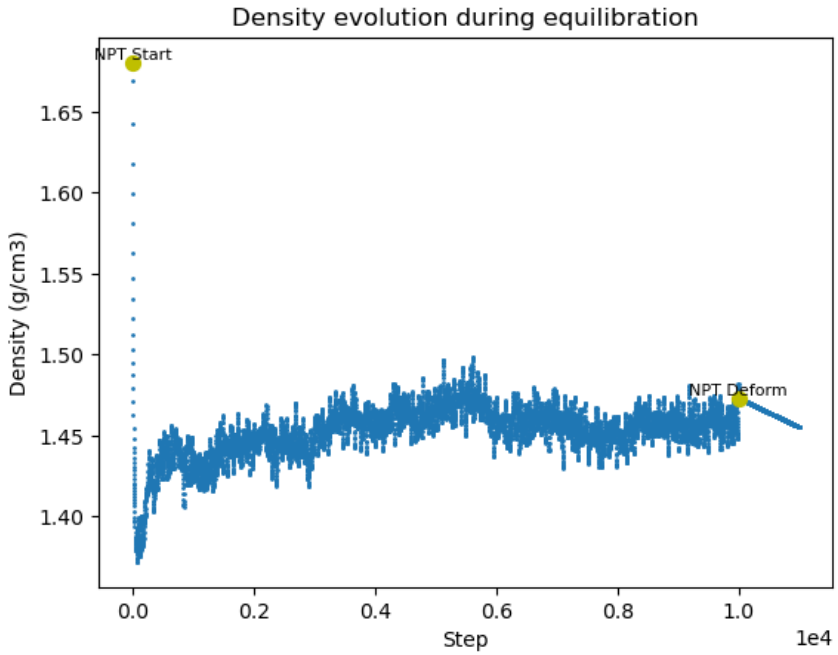

Figure 1.4: Density vs Runtime for the equilibration procedure

Following these equilibration steps, the simulations undergo another NVT to control the temperature - as done by the heat chamber in a Rheometer - while sinusoidally deforming the system at a user-defined amplitude, temperature, pressure, and frequency. At the time of publication, only the tensile/compressive and shear analyses are available, but we will be adding options for purely tensile, purely compressive, and cantilever perturbations in DMAx 2.0 as well as several other new features later described in the Future Work section.

The sample oscillatory process is different in DMAx from experiments in the sense that it simulates a user-defined strain and calculates the output stress while experiments do the exact opposite. However, since the relevant measure for property calculations is the phase lag between both signals, it does not matter which stimulus is applied and which is measured. Mechanical properties are then obtained from the MD trajectory of this oscillatory step in the simulation, where we use the *Scipy* Python package to fit a sinusoidal curve to the pressure output and

measure the phase angle between such fitted curve and the original strain applied. Although the Nyquist-Shannon [11] sampling theorem indicates that one should have at least double the sampling rate than the maximum frequency of the observed signal, we collect 1000 data points per sinusoidal cycle by default. We do so to ensure data fitting accuracy while not compromising simulation time.

The pressure data output from LAMMPS is a second rank tensor. Therefore, for compression/tension mode, the pressure sampled is parallel to the direction in which the strain is applied, while for shear mode, the pressure analyzed is perpendicular to the strain. For the compression/tension mode, we also ensure to expand/shrink the unit cell dimensions respectively as we strain the system in order to maintain a constant volume, which is crucial to mimic experimental results.

Strain Size Convergence

There is no clear consensus on the correct strain size to use in a material when simulating DMA, only recommendations that such value lies within the linear viscoelastic region of the material. This convergence step identifies the plastic transformation regime of the material and a consequent maximum allowed strain, an analysis that is standard in experimental DMA [12].

Another important aspect of this analysis which has not been previously discussed in the scarce computational DMA literature is the accuracy vs. cost-effectiveness of MD simulations with this type of sinusoidal perturbation. The thermostat coupled with the oscillatory command is known for yielding pressure oscillations [13] that, under low amplitudes, generate an unfilterable noise in the sinusoidal signal. This phenomenon is even more prominent in amorphous polymer systems in which the predominant van der Waals (vdW) interactions cannot counteract the strain as strongly as the directional covalent bonds in crystalline systems, yielding a pressure signal

that might be lower than the random oscillations caused by the thermostat. Such a behavior is depicted for amorphous PVDF in Figures 1.5 and 1.6.

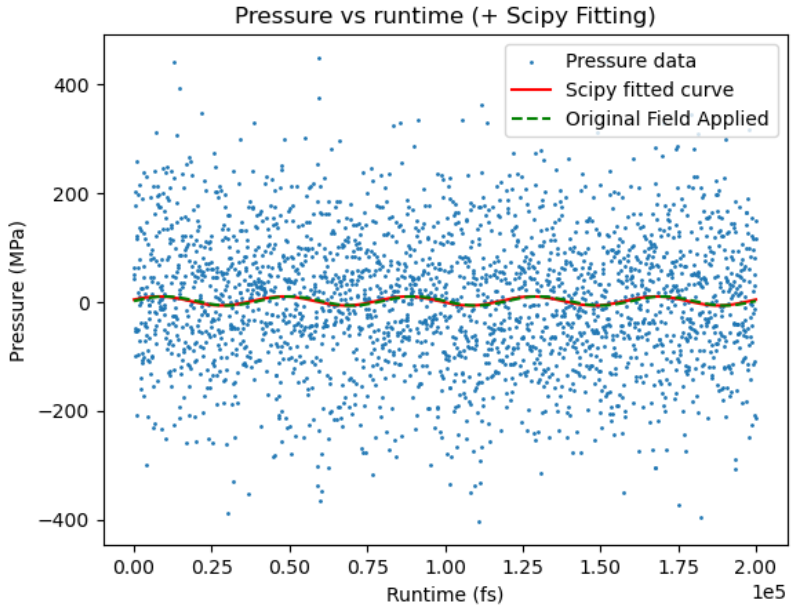

Figure 1.5: Pressure evolution over the perturbation step of the DMA analysis at 1% strain.

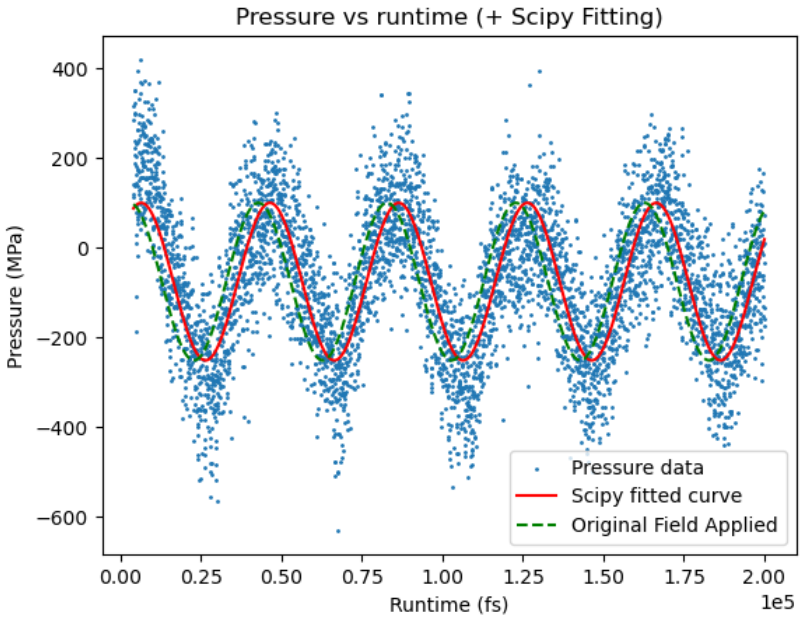

Figure 1.6: Pressure evolution over the perturbation step of the DMA analysis at 23% strain.

As aforementioned, such noise can be reduced by drastically expanding the system, but this can greatly increase the computational cost of simulations in the workflow. Therefore, our alternative to mitigate this noise is determining an optimal strain size besides the maximum one that minimizes a statistical cost function. This is also important in approximating, as much as possible, computational strain values to experimental ones, which are much lower for both crystalline and amorphous systems.

For the convergence analysis, structures undergo 10 DMA cycles with strain amplitudes between 0.1 and 50% (amorphous) or 0.001 and 10% (crystalline) the length of the unit cell. We then measure the SM, LM, and LT, as well as the Root-Mean-Squared Error (RMSE), R2-score, and offset from the original pressure in the sinusoidal curve fitting. We rank the data based on the lowest RMSE and offsets and highest R2 scores and the strain with the best summed score is selected to be used throughout the rest of the workflow. An example of such analysis for PVDF is shown in Figure 1.7. While the suggested strain in [7] is about 12%, our workflow indicates a better convergence over a strain of approximately 8%. That is due primarily to the high negative pressure offset at 12%, indicating that the system is undergoing a small drift, which is an error inherent to MD simulations over high perturbation.

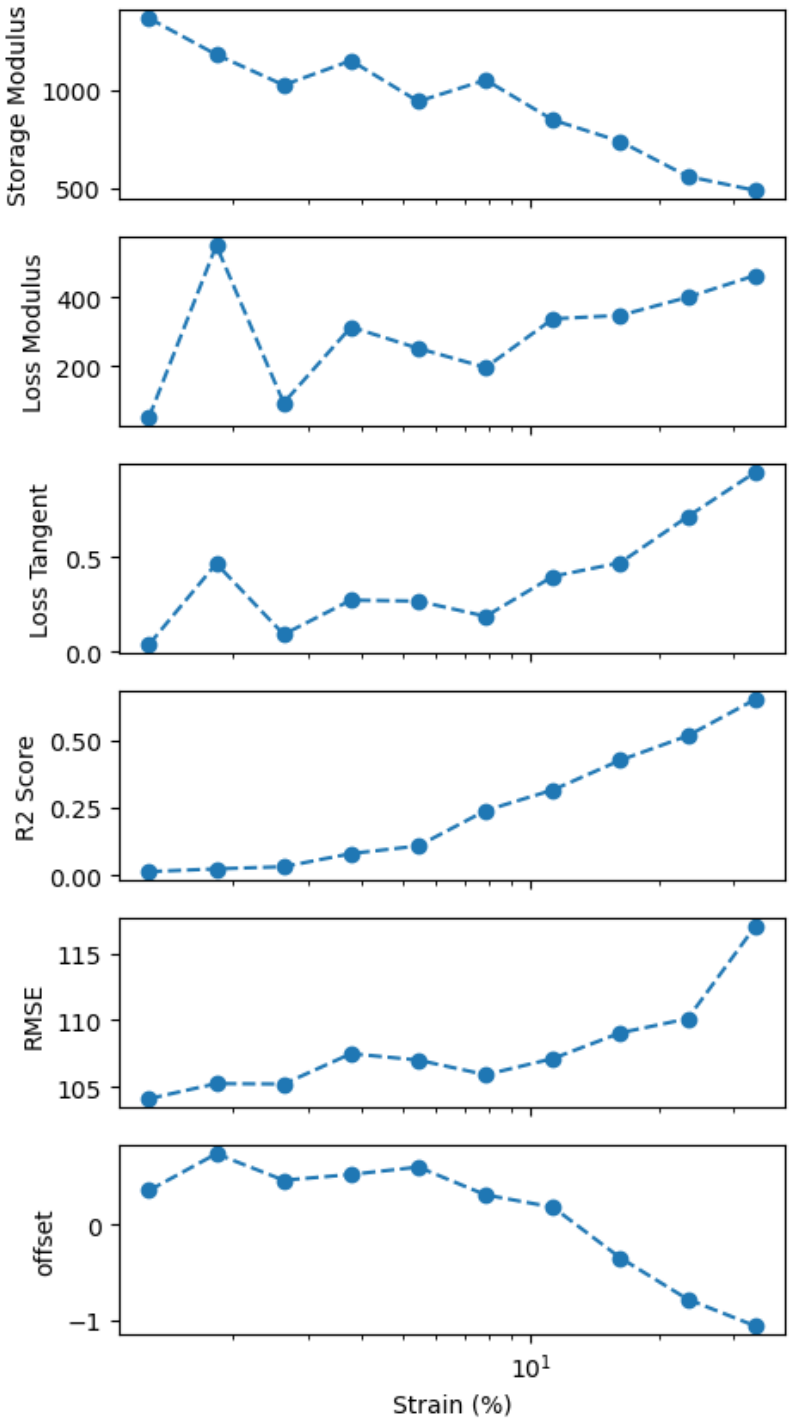

Figure 1.7: Output from the strain size convergence step of the workflow for amorphous PVDF. Measurable properties (SM, LM, and LT) are somewhat constant near the most appropriate strain size.

Number of Cycles Convergence

This convergence step was primarily designed to cut computational costs for the simulations and allow for a high-throughput analysis method. For the previous step of the workflow, 10 full cycles of DMA are run, and a sinusoidal curve is fit to such data. However, most times - especially for crystalline structures - much fewer cycles are usually necessary to obtain a good sinusoidal fitting. Additionally, despite being in the elastic regime of materials, continuous oscillations can slightly alter the hysteresis cycle in both experimental and computational settings as depicted in Figure 1.8. Therefore, with the newly determined optimal strain size, the 10-cycle simulation at that strain is cut into smaller outputs with 1 through 10 cycles. The R2-score is then determined for all numbers of cycles and convergence is achieved once the score varies less than 1% based on the previous result. A PVDF example of this workflow step is illustrated in Figure 1.9. The workflow convergence standards suggest 4 cycles for a 12% strain rather than the suggested 2 from [7], indicating that their data could have been slightly underfitted, thus yielding to less accurate SM, LM, and LT results.

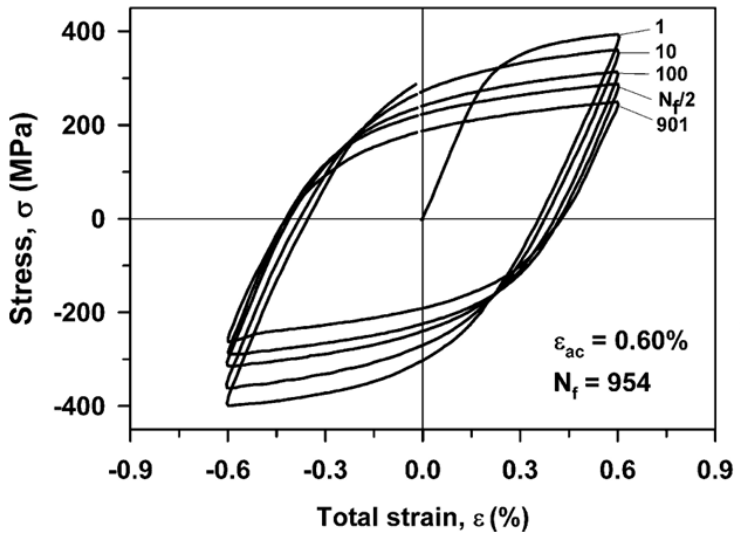

Figure 1.8: Hysteresis loop deviation over multiple DMA cycles. Adapted from [14]

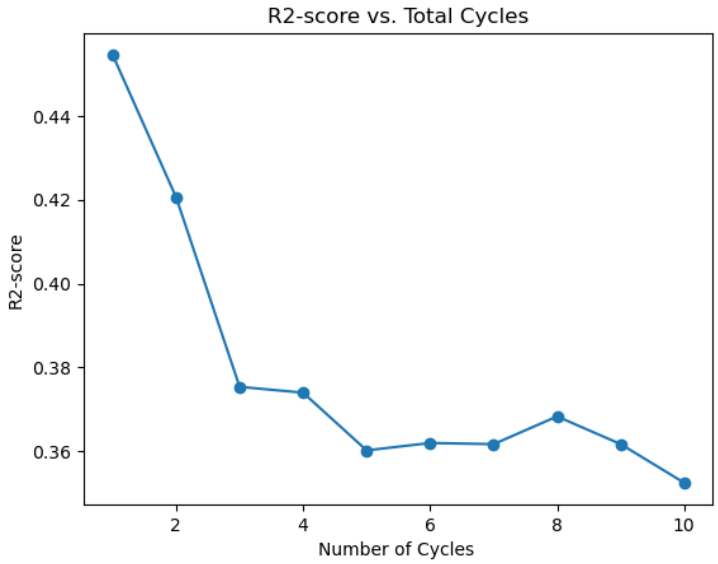

Figure 1.9: Runtime convergence plot for amorphous PVDF.

Error Analysis

This step of the workflow, as well as the rest of the tasks described, goes beyond any information previously provided in literature analyzing the cyclical mechanical properties of materials with MD. It utilizes the optimized strain size and number of cycles to determine the expected error in all simulations under these parameters.

Differently from all other simulations in the workflow, each dynamic oscillation is assigned a different Maxwell-Boltzmann distribution of the velocities at the desired analysis temperature, which otherwise is set to 300K. Such a process initiates at random velocity seeds, indicating different starting points for the structure. Since the structure utilized has been previously optimized in the workflow, we assume that it has equilibrated at the temperature of interest and that any random velocity distribution could converge to stable dynamics.

The error can be plotted at different frequencies such as in Figure 1.10, with a standard frequency of 25GHz. Such as in all other steps of the workflow, any simulation with an R2 score

lower than 0.01 is eliminated from the error analysis plot since the noise prevents the capture of a well-defined sinusoidal behavior, thus making the data unreliable.

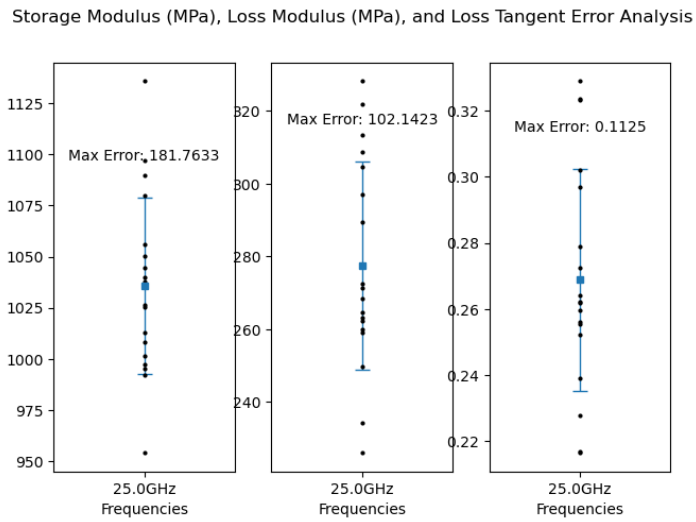

Figure 1.10: Error analysis for the SM, LM, and LT of amorphous PVDF.

Glass Temperature Analysis

The glass transition temperature (Tg) represents a critical thermodynamic property in amorphous polymers, delineating the transition from a rigid, glassy state to a more pliable, rubbery state. This temperature point, crucial in understanding the material's behavior, signifies the change in molecular mobility without a distinct phase transition. Below Tg, polymers exhibit a solid, vitreous state characterized by restricted molecular motion and high stiffness, while above this threshold, increased molecular mobility results in a more flexible, rubbery behavior. The value of Tg is influenced by various factors, including molecular weight, chain flexibility, chemical structure, and processing conditions. Accurate determination and comprehension of Tg are paramount for tailoring polymer properties to specific applications, impacting material design, processing techniques, and performance in various industries [15].

In our workflow, we encoded the first glass temperature analysis method utilizing computational DMA to date. Current methods for determining this polymeric property rely on a long and expensive set of simulations in which the system volume is equilibrated with an NPT ensemble under different temperatures, as done at the structure equilibration step in DMAx. In our case, we assume that, even though deviating from expected system density for other data points, a single equilibration step at room temperature is enough for the structure as long as the velocities are reassigned at the oscillatory step to match the desired temperature of observation. The set of simulations for DMAx are much shorter than the aforementioned NPT method since higher frequencies translate into shorter periods, hence shorter runtimes for the oscillatory runs.

Figure 1.11 shows the fitted LT evolution for the PVDF system at 5GHz between -80°C and 80°C, sampled at a 1°C rate. When compared to Figure 1.12, which portraits experimental data for the same system, one notices that the simulated and experimental glass transition temperature ranges match, with a difference in the peak Tg of about 3°C. Further information about the glass temperature of the sample, including the comparison of SM data with experiments and explanations about data variation with frequency, is detailed in the Results chapter.

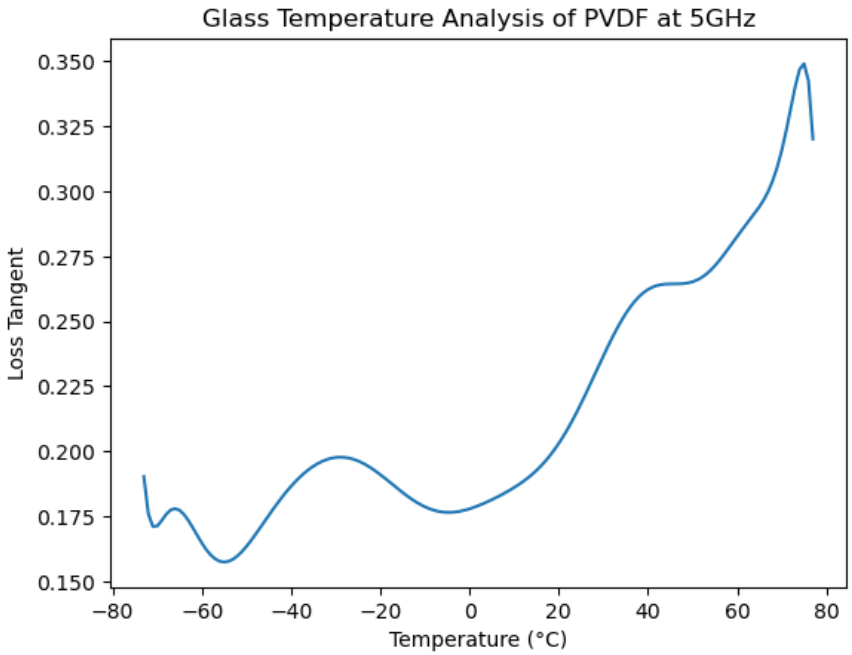

Figure 1.11: Glass Temperature Analysis of PVDF at 5GHz

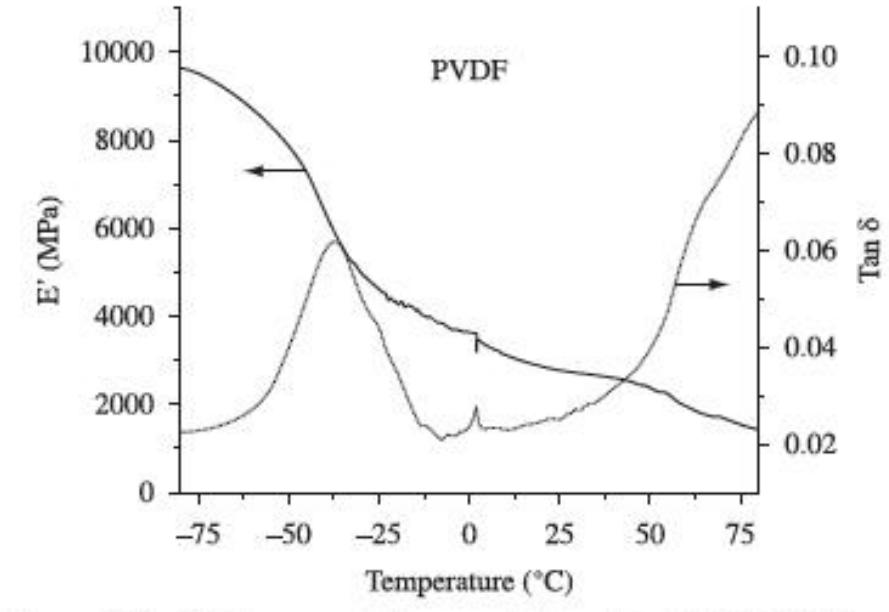

Figure 1.12: Experimental SM and LT of PVDF. Adapted from [16]

Master Curve

Like the glass transition temperature, Master Curves (MCs) are of ultimate importance for the characterization of polymers. They aid in extrapolating material behavior under conditions that might not be practically feasible to test in a laboratory setting, offering invaluable insights into the mechanical behavior of polymers across diverse environmental conditions. The Time-Temperature Superposition (TTS) principle forms the basis for constructing Master Curves (MCs) in polymer characterization. It postulates that different experimental data obtained at various temperatures and time scales can be shifted and superimposed onto a single master curve by using a time-temperature shift factor. This shift factor allows the rearrangement of the data to align with a reference temperature or time, typically the glass transition temperature or the characteristic relaxation time. By applying appropriate shifts along the frequency and temperature axes, the viscoelastic behavior observed at different conditions can be unified onto a single master curve, providing a comprehensive depiction of the material's mechanical response across a broader range of temperatures and frequencies.

As observed in Figure 1.13, the storage modulus (E') is plotted against a frequency or time window over several isotherms. Each isotherm is then assigned a temperature-dependent shift factor α with respect to the intermediate temperature (T_0) of the dataset, which can either be determined by computational curve fitting methods or based on the experimental Williams-Landel-Ferry (WLF) equation (Equation 2).

$$\log(\alpha) = \frac{C1*(T-T_0)}{C2+(T-T_0)} \quad \text{(Equation 2)}$$

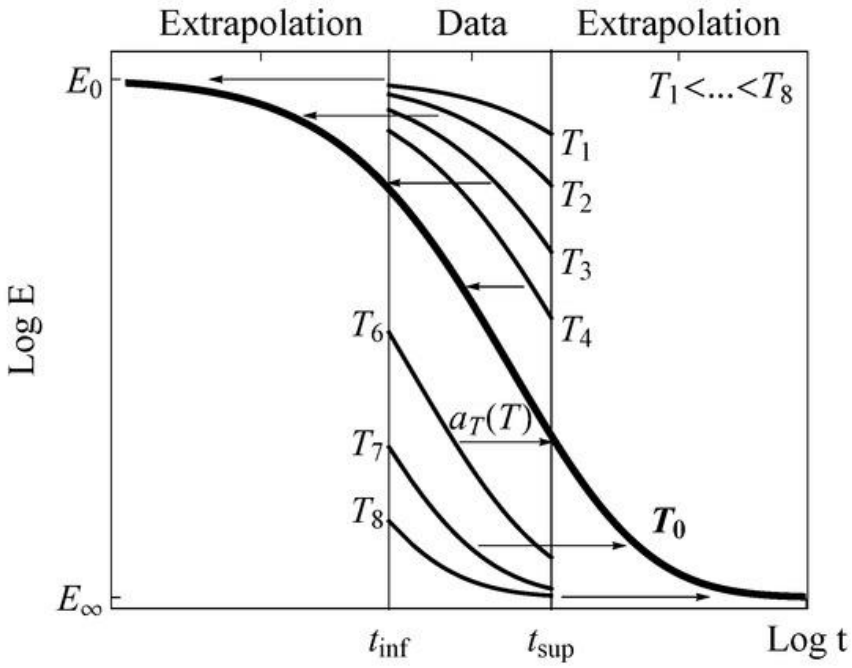

Figure 1.13: Master Curve fitting procedure. Adapted from [6]

The WLF method relies on two material-specific constants, C_1 and C_2, which will likely not be available for all polymers studied with DMAx. Therefore, we opt for a curve-fitting approach by using [17]'s *mastercurves* Python package. This software utilizes a Gaussian Process Regression (GPR), which is a machine learning method, for determining the shift factors and creating a continuous curve based on the reference temperature. It predicts a smooth interpolant with its respective uncertainty bounds that will be responsible for assigning vertical and horizontal shifts to each isotherm that ensure maximum possible continuity of the final MC. The final plot should then have data for the mechanical response of the material at the intermediary temperature of the dataset - usually the glass transition temperature - over a much broader frequency range. The example for PVDF will be further discussed in the Results section.

Acknowledgements

Chapter 1, in full, is currently being prepared for submission for publication of the material. Silva Buarque, Ricardo; Fune, Beneen; Jamnuch, Sasawat; Ravisankar, Aishwarya; Pascal, Tod. The thesis author was the primary researcher and author of this material.

Chapter 2 Results, Limitations & Future Work

In this chapter, we hope to elaborate on the data comparison made with [7] to validate our DMAx's method. In addition, we introduce more details on the error and glass temperature analyses as well as on the master curve construction for the PVDF system. We hope to elucidate the quality of the data by comparing it to experimental results as well as indicate limitations of it and improvements already planned for DMAx 2.0.

Table 2.1 displays the SM, LM, and LT values obtained by DMAx and by [7] for an equivalent PVDF system under the frequencies of 0.25GHz, 2.5GHz, and 25GHz and at 12.5% strain over only 2 oscillations, closely matching Ghajar's simulation conditions. We observe that most data points disagree by more than the expected error margin for DMAx results at 25 GHz depicted in the previous chapter. The data at lower frequencies tends to deviate even more from our calculations and at what we argue to be an incorrect trend for this type of material.

Table 2.1: Values of SM, LM, and LT calculated with DMAx and by Ghajar et. Al.

	DMAx	**Ghajar et. Al.**
0.25 GHz	SM: 928 MPa, LM: 205 MPa, LT: 0.22	SM: 602 MPa, LM: 709 MPa, LT: 1.178
2.5 GHz	SM: 718 MPa, LM: 270 MPa, LT: 0.37	SM: 825 MPa, LM: 669 MPa, LT: 0.811
25 GHz	SM: 966 MPa, LM: 367 MPa, LT: 0.38	SM: 1761 MPa, LM: 748 MPa, LT: 0.424

For most polymers and, specifically, for PVDF as depicted in Figures 2.1 and 2.2, the SM typically tends to increase or remain the same while the LT mostly increases with an increase in frequency. This indicates that the phase angle between the simulated strain and computed stress increases, also highlighting that the material becomes more lossy. [18] explains that higher frequencies constraint the flow of the polymer chains, thus increasing heat losses as bonds are

not able to absorb the input energy at the appropriate relaxation time. Additionally, an argument could be made about higher frequencies exciting new vibrational modes on the structure which could generate more thermal losses.

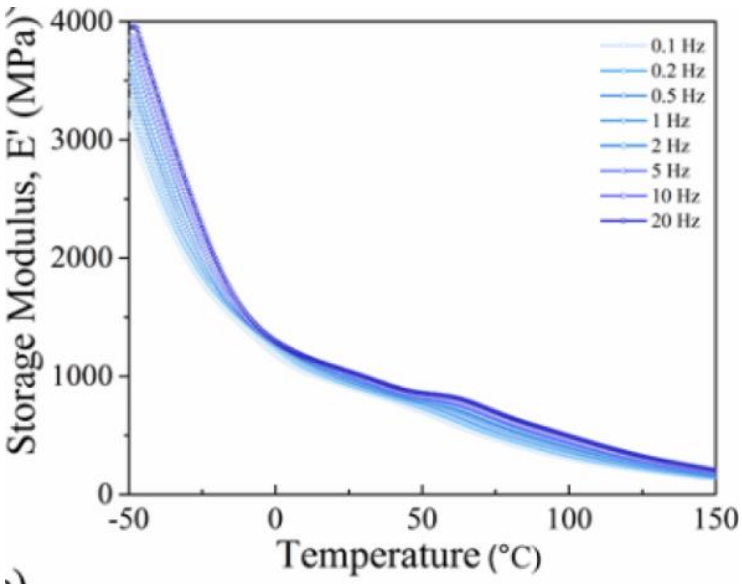

Figure 2.1: SM evolution of PVDF at different experimental frequencies. Adapted from [19]

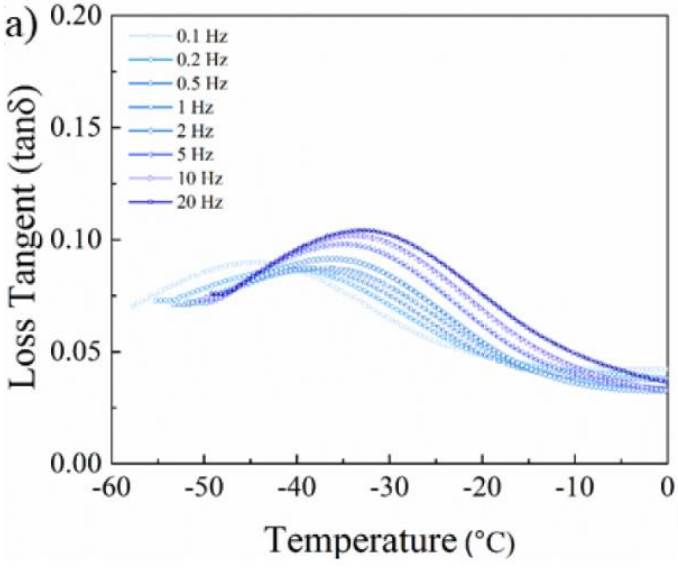

Figure 2.2: LT evolution of PVDF at different experimental frequencies. Adapted from [19]

Even though the SM data at 2.5 GHz is lower than that of 0.25GHz, the discrepancy lies within the error margin at this frequency and temperature and the expected data trend is in great agreement with DMAx results, supporting the conclusion that there could be incorrect physics encoded in the DMA simulations of Ghajar's work. Alternatively, Ghajar's data could be affected by the construction mechanism of the amorphous structure as well as by the fitting quality of the sinusoidal data. As aforementioned, we ensure to collect at least 1000 data points per cycle to account for the high-pressure fluctuations of MD, but there is no reference regarding the sampling rate of [7].

Another factor that validates the quality of our data is the close match between the Young's modulus calculated with our system in comparison to that of an amorphous PVDF experimental sample. When the sinusoidal curve is fit to the pressure data through time, we can plot that series of data points against the associated strain applied at the simulation timestep when each pressure was computed. Since we ensure that the material is within its elastic deformation regime, the slope of the longest axis of the plotted ellipsoid should be equal to the Young's modulus of the system [7]. For PVDF at 25GHz with the OPLS-AA FF, we calculate a Young's modulus of 1065.33 MPa, which is close to the experimental value of 1260 MPa [20], especially taking into account the large pressure fluctuations for the amorphous system. The ellipsoid for this calculation is depicted in Figure 2.3.

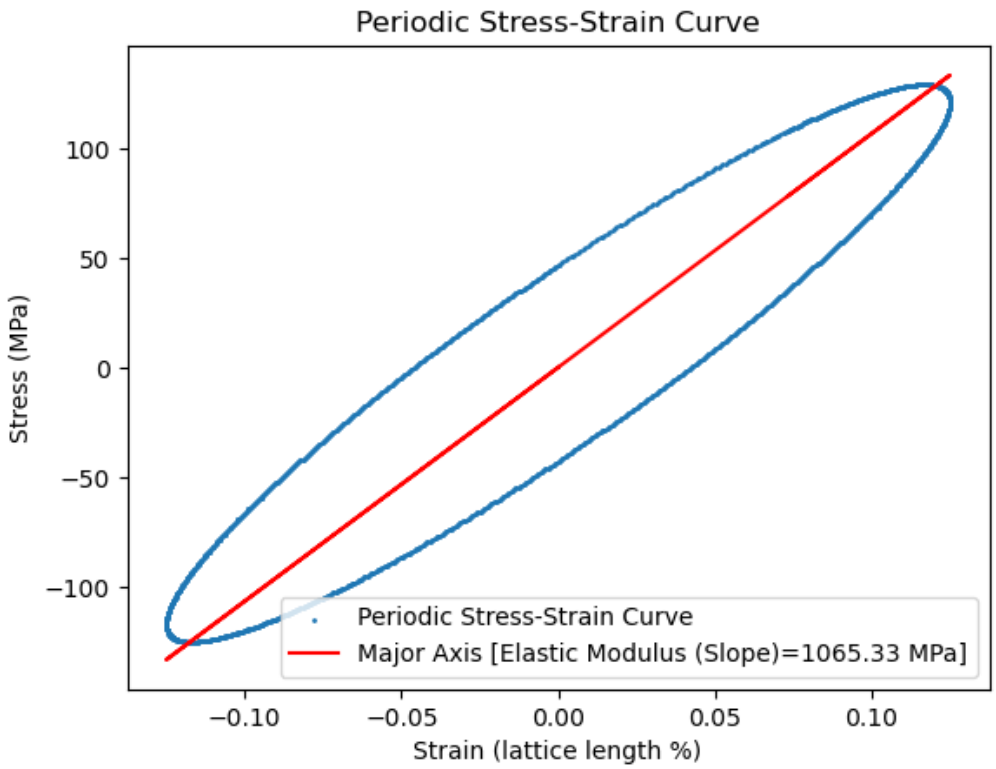

Figure 2.3: Periodic stress-strain curve of amorphous PVDF with the OPLS-AA forcefield and fitted Young's Modulus.

We further elucidate the quality and limitations of our data by extending our observation over the Tg results. Figure 2.4 plots the SM, LM, and LT data points – rather than the smoothed curve presented in Chapter 1 – for the PVDF sample at 5GHz with the OPLS-AA FF. Despite the great agreement of the glass transition regime with experimental data, we must highlight that the SM and LM data do not match expected experimental values, for which SM below the Tg regime is expected to increase much more rapidly as depicted in Chapter 1. As the polymer becomes crystalline, the LM is also expected to decrease, a fact that is not observed in our data set.

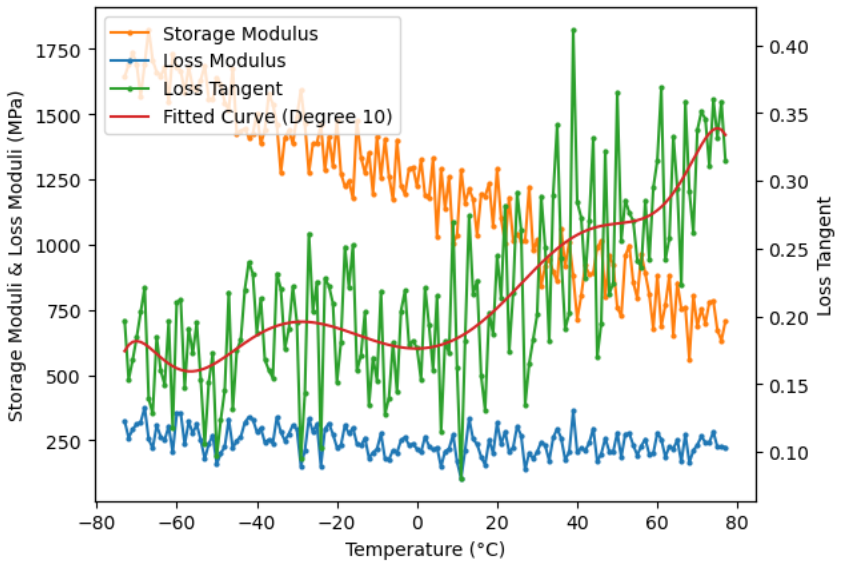

Figure 2.4: SM, LM, and LT for PVDF at 5GHz near Tg

This disagreement is mostly due to the lack of any crystallinity on the structure studied, which also greatly affects the noise in the data, leading to a potential argument that the fitted glass transition regime has too much error to be considered a peak. The optimal approach for this matter would be to simulate a semicrystalline system at the glass temperature regime, a crystalline structure below Tg and the purely amorphous one after this range, weighting the data from all within the total temperature range to account for the appropriate dynamics at each regime. However, we have not yet successfully been able to develop an accurate semicrystalline structure or a crystalline one with comparable box dimensions and chain sizes.

In addition, this workflow is intended to be useful for any polymer despite prior experimental knowledge, thus allowing for new compositions and novel structures. With this in mind, we are still not able to automatically determine the temperature range in which the glass transition should occur, having relied on experimental data values to decide on the temperature range of our simulations.

For the subsequent version of DMAx, we are integrating [21]'s workflow for generating semicrystalline polymer structures as well as an in-house script to adapt fully crystalline structures to similar dimensions as that of the semicrystalline and amorphous systems studied near Tg. In addition, we will incorporate [22]'s 2-Phase Thermodynamics (2PT) code in our workflow to screen the Gibbs Free Energy curves of each structure and determine the appropriate temperature ranges to simulate the phase transition. Since 2PT relies on even shorter simulation times, we will be able to make a refined analysis even over a broader temperature range.

We conclude our data analysis by commenting on the results of the Master Curve obtained for the PVDF system with the OPLS-AA FF. This analysis contains data of 100 simulations at frequencies varying between 10 and 100GHz and temperatures between -70°C and 20°C, encompassing the glass transition region of this polymer with the Tg at the center point of all measurements. Figures 2.5 – 2.7 portray SM, LM, and LT data associated with the construction of the master curves for PVDF. The top plots depict the original data points collected at the previously referenced frequencies and temperatures. The middle graphs depict the curves fit to each isotherm and the interpolant error margins for the data. Finally, the last plots portray the actual MCs for SM, LM, and LT respectively, composed of the shifted data from all isotherms.

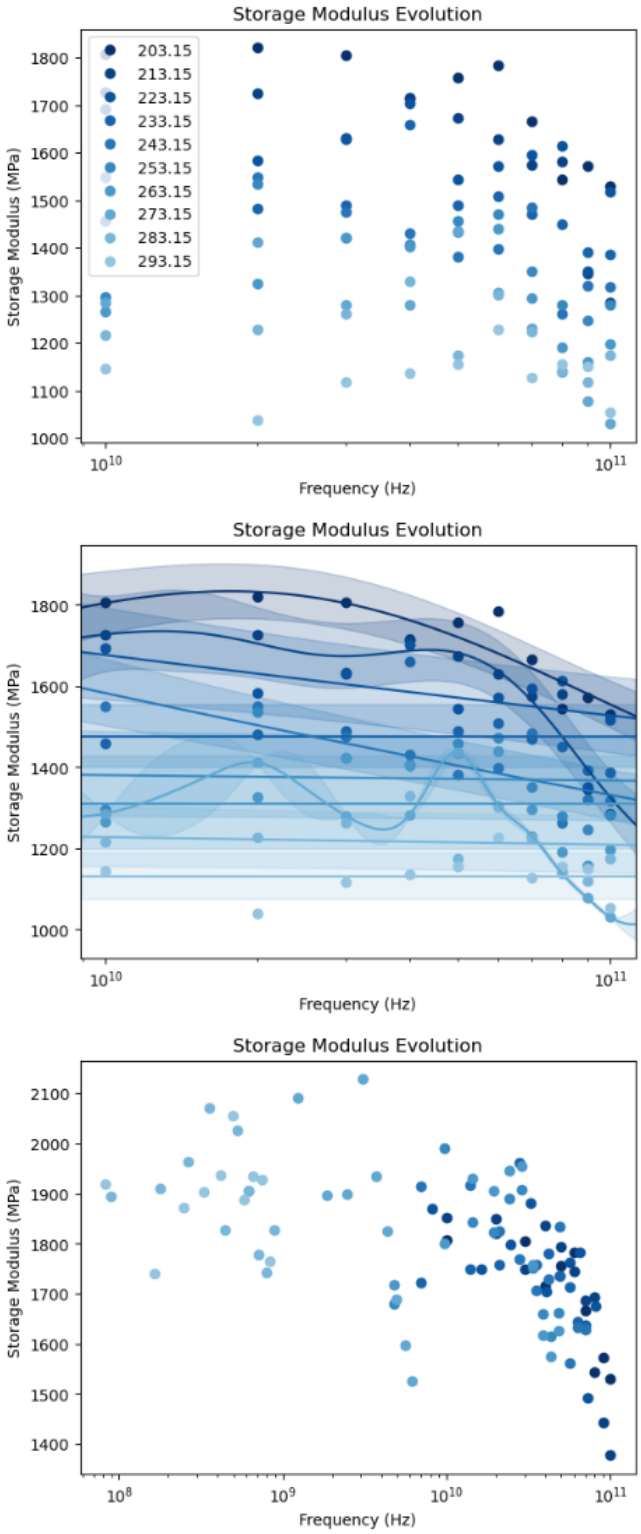

Figure 2.5: Storage Modulus MC data

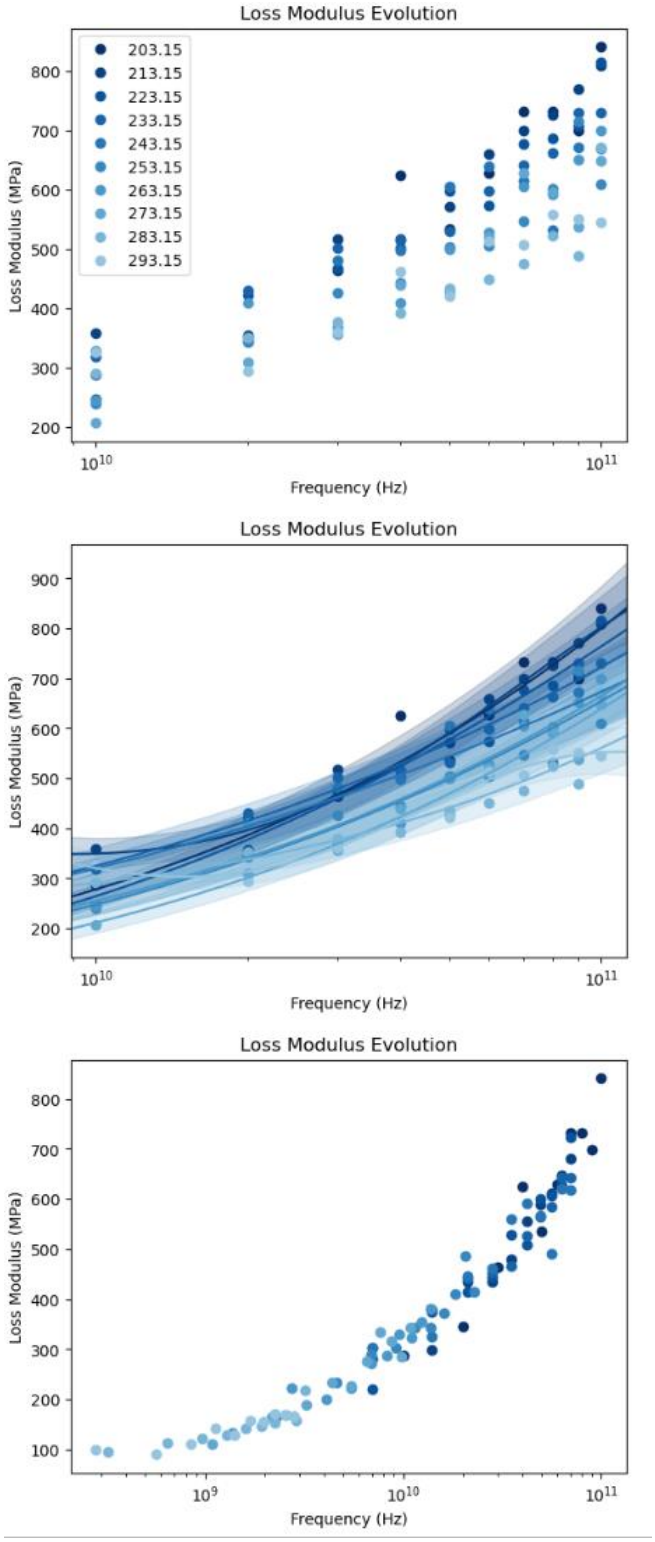

Figure 2.6: Loss Modulus MC data

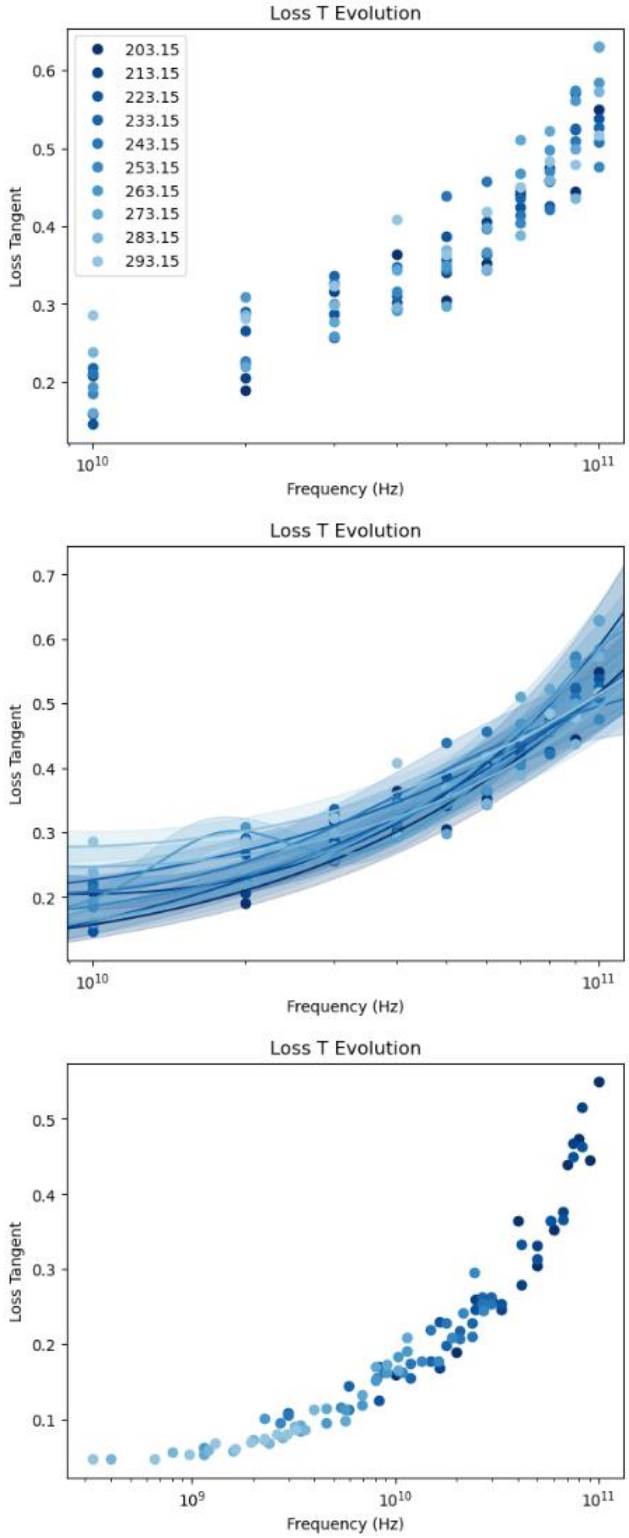

Figure 2.7: Loss Tangent MC data

In comparing the new low-frequency data and extrapolating its trend to even lower frequencies, we notice that both the SM and LT data closely match the experimental values from Figures 2.2 and 2.3 within the error margins of DMAx. We can further prove from this analysis that the SM remains mostly constant even through such a high frequency range while the LM and LT increase with reduced oscillation periods. We also observe a decreasing trend for the SM above the GHz regime, which is mostly attributed to the lower SM data computed for the highest frequencies in the original data set. However, this data is known to be less reliable as, for higher frequencies, the mechanical signal begins to couple with the temperature update frequency, leading to unstable dynamics. We also must highlight that the lack of crystallinity in the system could be greatly impacting the data quality at temperatures below Tg.

For DMAx 2.0, besides the aforementioned updates, we hope to add better convergence metrics for the MC to ensure its data reliability as well as a machine-learned universal forcefield for polymers with polarizable charges. This will drastically improve data accuracy as it will allow for better resolution on vdW interactions, which are the primary forces acting upon polymeric systems. Additionally, it will enable charge reparameterization as molecules oscillate in distance due to the periodic oscillation of the system.

Acknowledgements

Chapter 2, in full, is currently being prepared for submission for publication of the material. Silva Buarque, Ricardo; Fune, Beneen; Jamnuch, Sasawat; Ravisankar, Aishwarya; Pascal, Tod. The thesis author was the primary researcher and author of this material.

CONCLUSION

We have developed a first-of-its-kind platform for computing dynamic mechanical properties of materials. Our workflow is capable of calculating the Young's Modulus, Storage Modulus, Loss Modulus, and Glass Transition Temperature of a material with as little as a SMILES string utilized to generate the structure, making the software extremely user-friendly. We also offer an error analysis metric to determine the quality of each system's data. Besides the glass temperature – greatly affected by the data error margins and by the lack of crystallinity in the current system – our other simulated properties greatly match experimental values. In fact, we are able to compute a master curve by obtaining DMA data at multiple frequencies and temperatures and the extrapolated values closely match the SM and LT observed at the low-frequency regime in experiments.

DMAx 1.0, our Python package, is available free of charge on our GitHub repository (https://github.com/rsilvabuarque/DMAx). An upgraded version of this workflow is already under development for future publication and will contain several improvements focused on structure generation and data quality assurance. We hope to stem from pre-built algorithms capable of generating accurate crystalline and semicrystalline polymer structures to better understand the materials behavior near the glass transition regime. We also plan to integrate a computationally inexpensive Gibbs Free Energy analysis of the crystalline, semicrystalline, and amorphous systems over a large range of temperatures to define the range in which the glass temperature should be computed with DMA calculations. Finally, we are developing a universal machine-learned polymer forcefield with polarizable charges to better determine the atom dynamics in the system and minimize the pressure fluctuations.

REFERENCES

[1] M. Sepe, “Part 5: Heat deflection temperature vs. dynamic mechanical analysis,” Plastics Technology, https://www.ptonline.com/articles/part-5-heat-deflection-temperature-vs-dynamic-mechanical-analysis (accessed Dec. 6, 2023).

[2] D. Jones, “Dynamic mechanical analysis of polymeric systems of pharmaceutical and biomedical significance,” *International Journal of Pharmaceutics*, vol. 179, no. 2, pp. 167–178, 1999. doi:10.1016/s0378-5173(98)00337-8

[3] M. Oregui, A. de Man, M. F. Woldekidan, Z. Li, and R. Dollevoet, “Obtaining railpad properties via dynamic mechanical analysis,” *Journal of Sound and Vibration*, vol. 363, pp. 460–472, 2016. doi:10.1016/j.jsv.2015.11.009

[4] N. Huebsch, C. Kearney, X. Zhao, J. Kim, C. Cezar, Z. Suo, D. Mooney, “Ultrasound-triggered disruption and self-healing of reversibly cross-linked hydrogels for drug delivery and enhanced chemotherapy,” *Proceedings of the National Academy of Sciences*, vol. 111, no. 27, pp. 9762–9767, 2014. doi:10.1073/pnas.1405469111

[5] F. Lionetto, F. Montagna, and A. Maffezzoli, “Ultrasonic dynamic mechanical analysis of polymers,” *Applied Rheology*, vol. 15, no. 5, pp. 326–335, 2005. doi:10.1515/arh-2005-0016

[6] A. Álvarez-Vázquez, A. Fernández-Canteli, E. Castillo Ron, P. Fernández Fernández, M. Muñiz-Calvente, M. Lamela Rey, “A novel approach to describe the time–temperature conversion among relaxation curves of viscoelastic materials,” *Materials*, vol. 13, no. 8, p. 1809, 2020. doi:10.3390/ma13081809

[7] M. H. Ghajar, M. Mosavi Mashhadi, and H. Ghattan Kashani, “Dynamic mechanical analysis of Bucky Gel actuator electrolyte by molecular dynamics simulation,” *Computational Materials Science*, vol. 149, pp. 379–385, 2018. doi:10.1016/j.commatsci.2018.03.050

[8] S. Ebnesajjad, “Fluoropolymers: Properties and structure,” *Melt Processible Fluoroplastics*, pp. 9–21, 2003. doi:10.1016/b978-188420796-9.50005-9

[9] R. G. Kepler and R. A. Anderson, “Piezoelectricity and pyroelectricity in polyvinylidene fluoride,” *Journal of Applied Physics*, vol. 49, no. 8, pp. 4490–4494, 1978. doi:10.1063/1.325454

[10] H. Sahu, K.-H. Shen, J. H. Montoya, H. Tran, and R. Ramprasad, “Polymer structure predictor (PSP): A python toolkit for predicting atomic-level structural models for a range of polymer geometries,” *Journal of Chemical Theory and Computation*, vol. 18, no. 4, pp. 2737–2748, 2022. doi:10.1021/acs.jctc.2c00022

[11] C. L. Farrow, M. Shaw, H. Kim, P. Juhás, and S. J. Billinge, “Nyquist-Shannon sampling theorem applied to refinements of the atomic pair distribution function,” *Physical Review B*, vol. 84, no. 13, 2011. doi:10.1103/physrevb.84.134105

[12] K. P. Menard and N. Menard, *Dynamic Mechanical Analysis*. Boca Raton, FL: CRC Press, 2020.

[13] S. E. Feller, Y. Zhang, R. W. Pastor, and B. R. Brooks, “Constant pressure molecular dynamics simulation: The Langevin Piston Method,” *The Journal of Chemical Physics*, vol. 103, no. 11, pp. 4613–4621, 1995. doi:10.1063/1.470648

[14] R. Mishnev, N. Dudova, and R. Kaibyshev, “Low cycle fatigue behavior of a 10% CR martensitic steel at 600°C,” *ISIJ International*, vol. 55, no. 11, pp. 2469–2476, 2015. doi:10.2355/isijinternational.isijint-2015-336

[15] B. R. Bhandari and T. Howes, “Implication of glass transition for the drying and stability of dried foods,” *Journal of Food Engineering*, vol. 40, no. 1–2, pp. 71–79, 1999. doi:10.1016/s0260-8774(99)00039-4

[16] L. F. Malmonge, S. do Langiano, J. M. Cordeiro, L. H. Mattoso, and J. A. Malmonge, “Thermal and mechanical properties of PVDF/Pani blends,” *Materials Research*, vol. 13, no. 4, pp. 465–470, 2010. doi:10.1590/s1516-14392010000400007

[17] K. R. Lennon, G. H. McKinley, and J. W. Swan, “A data-driven method for automated data superposition with applications in soft matter science,” *Data-Centric Engineering*, vol. 4, 2023. doi:10.1017/dce.2023.3

[18] J. C. Duncan and D. M. Price, “Thermomechanical, dynamic mechanical and dielectric methods,” *Principles of Thermal Analysis and Calorimetry*, pp. 164–213, 2016. doi:10.1039/bk9781782620518-00164

[19] F. Mokhtari, G. M. Spinks, S. Sayyar, and J. Foroughi, “Dynamic mechanical and creep behaviour of meltspun PVDF nanocomposite fibers,” *Nanomaterials*, vol. 11, no. 8, p. 2153, 2021. doi:10.3390/nano11082153

[20] A. Mandal and A. K. Nandi, “Physical properties of poly(vinylidene fluoride) composites with polymer functionalized multiwalled carbon nanotubes using nitrene chemistry,” *Journal of Materials Chemistry*, vol. 21, no. 39, p. 15752, 2011. doi:10.1039/c1jm12926k

[21] B. Belin, M. Yiannourakou, V. Lachet, and B. Rousseau, “Modeling method for semicrystalline polymers controlling aspects of the morphology at the molecular scale for the study of mechanical and physicochemical properties,” *The Journal of Physical Chemistry B*, vol. 126, no. 46, pp. 9673–9685, 2022. doi:10.1021/acs.jpcb.2c04571

[22] S.-T. Lin, P. K. Maiti, and W. A. Goddard, “Two-phase thermodynamic model for efficient and accurate absolute entropy of water from molecular dynamics simulations,” *The Journal of Physical Chemistry B*, vol. 114, no. 24, pp. 8191–8198, 2010. doi:10.1021/jp103120q